Academic Journal of Science and Technology
ISSN: 2771-3032 | Vol. 23, No. 2, 2026

Shixiaosan Attenuates Intestinal Epithelial Barrier Injury in TNF-α-stimulated Caco-2 Cells and DSS-induced Colitis Mice

Tianyu She[1, *], Bei Huang[2, *], Yunlong Gao[3], Weiling Liu[4], Wenjing Yan[5], Qiyi Hu[6], Xiaoying Tian[1], Xiaoxiao Zhao[7], Yina Zhao[1], Hangyan Qian[8], Na Jing[9], Yuan Wang[10], Dan Yun[11]

[1]Department of Medical Imaging Function, Xi'an Electric Power Central Hospital, Xi'an 710032, Shaanxi, China;
[2]Department of Anorectal, Xi'an Hospital of Traditional Chinese Medicine, Xi'an 710021, Shaanxi, China;
[3]The Second Affiliated Hospital of Xi'an Jiaotong University, Xi'an 710004, Shaanxi, China;
[4]Department of Colorectal Medicine, Affiliated Hospital of Shanxi University of Traditional Chinese Medicine, Taiyuan 030024, Shanxi, China;
[5]State Key Laboratory of Active Components and Pharmacodynamics of Natural Medicines, China Pharmaceutical University, Nanjing 210009, Jiangsu, China;
[6]Third People's Hospital of Beichuan Qiang Autonomous County, Mianyang 622750, Sichuan, China;
[7]Department of Traditional Chinese Medicine, Xi'an Electric Power Central Hospital, Xi'an 710032, Shaanxi, China;
[8]Department of Nursing, Xi'an Electric Power Central Hospital, Xi'an 710032, Shaanxi, China;
[9]Department of Thyroid and Breast Surgery, Xi'an Electric Power Central Hospital, Xi'an 710032, Shaanxi, China;
[10]People's Hospital of Yaozhou District, Tongchuan 727100, Shaanxi, China;
[11]Department of Proctology, Xi'an Electric Power Central Hospital, Xi'an 710032, Shaanxi, China.

*These authors contributed equally to this work.

Correspondence: Tianyu She (tianyu202210@126.com)

Abstract: Disruption of the intestinal epithelial barrier is implicated in the development and persistence of inflammatory bowel disease. Although Shixiaosan (SXS) has anti-inflammatory activity, its effects on epithelial barrier injury and the signaling events involved remain insufficiently characterized. We examined SXS in Caco-2 cells challenged with TNF-α and in mice with DSS-induced colitis, focusing on RELA/NF-κB signaling and myosin light-chain (MLC) phosphorylation. Cell experiments used SXS at 25–100 μg/mL and assessed viability, transepithelial electrical resistance (TEER), paracellular tracer flux, inflammatory mediators, and tight-junction proteins. Male C57BL/6 mice received 3% DSS for 7 days and regular water for a further 3 days, together with SXS at 1, 2, or 4 g/kg/day (n = 6 per group). Disease activity, tissue injury, serum barrier-related markers, inflammatory mediators, and colonic tight-junction proteins were evaluated. RELA silencing in the cell model was used to examine pathway involvement. SXS showed no obvious cytotoxicity and counteracted the TNF-α-associated loss of viability and TEER, limited paracellular permeability and inflammatory mediator release, and restored ZO-1, occludin, and claudin-1. In mice, treatment attenuated weight loss, disease activity, histological injury, and colon shortening, while lowering serum permeability markers and restoring colonic tight-junction proteins. Reduced phosphorylation of p65, IκBα, and MLC accompanied these protective effects. RELA knockdown also reduced MLC phosphorylation and partly recovered tight-junction protein expression. Together, these findings indicate that SXS limits experimental intestinal barrier injury and inflammation, with RELA/NF-κB-associated MLC phosphorylation implicated in its effects. Direct validation of MLCK remains necessary.

Keywords: Shixiaosan; Colitis; Intestinal mucosa; Tight junctions; NF-κB.

1. Introduction

Tight junctions between intestinal epithelial cells regulate paracellular passage and help prevent microorganisms and toxins in the lumen from entering underlying tissues. When this barrier is compromised, luminal molecules and microbial metabolites gain greater access to the mucosa, where they can provoke inflammation and tissue injury. The resulting increase in permeability is therefore an important contributor to colitis and other forms of inflammatory bowel disease [1].

Inflammatory activity can itself impair the intestinal epithelium. In experimental colitis, pronounced pro-inflammatory responses often coincide with epithelial damage, greater permeability, and altered tight-junction protein expression. TNF-α is one mediator of this injury [2]: it promotes inflammatory responses while also disrupting junctional organization and increasing paracellular passage. These effects make TNF-α useful for modeling epithelial barrier damage in cell culture. Typical responses include a fall in transepithelial electrical resistance, increased tracer transport between cells, and reduced ZO-1, occludin, and claudin-1, resembling changes observed in inflamed intestinal tissue.

The assembly, localization, and stability of tight junctions depend on coordinated interactions between junctional proteins and intracellular signaling systems [3]. NF-κB is involved in the epithelial response to inflammatory stimuli. Activation of this signaling axis can promote cytokine production and may enhance signaling involving myosin light chain kinase (MLCK), thereby enhancing myosin light chain phosphorylation and cytoskeletal tension. Such changes can destabilize junctional structures, making NF-κB/MLCK signaling a potential link between inflammation and structural barrier injury. Suppression of this pathway, together with restoration of tight-junction organization, may therefore help limit inflammation-related intestinal damage.

Shixiaosan (SXS) combines Cattail Pollen with Faeces Trogopteri and has been studied for a range of pharmacological effects. Whether this traditional Chinese medicine formula preserves the intestinal epithelial barrier during inflammation, however, remains insufficiently understood.

We investigated SXS in two complementary settings: DSS-induced colitis in mice and TNF-α-induced injury in intestinal epithelial cells. The study examined barrier function and tight-junction stability, with particular attention to the possible involvement of NF-κB/MLCK-related signaling [4]. The experiments indicated that SXS reduced inflammatory intestinal injury and improved epithelial barrier integrity.

2. Materials and Methods

2.1. Materials and reagents

To prepare SXS, 50 g each of Faeces Trogopteri and Cattail Pollen were combined and subjected to two 2-h reflux extractions with 1000 mL of yellow rice wine [5]. This solvent was chosen to reproduce the traditional wine-assisted preparation. Its aqueous component and low ethanol content may also aid the recovery of water-soluble and moderately polar compounds, including flavonoids and phenolic acids, from the two crude drugs. After pooling and filtration, the extracts were concentrated under reduced pressure to a crude drug-equivalent concentration of 0.12 g/mL for use in the experiments. Preliminary chemical quality confirmation used commercially purchased standards representing constituents of both ingredients [6]. Comprehensive HPLC–Q-TOF–MS profiling was outside the main scope of this work; detailed chromatographic results and MS/MS characterization are therefore not presented here.

Aliquots of the concentrated extract were kept at −20 °C and handled to avoid repeated freezing and thawing [7]. For each cell experiment, an aliquot was thawed just before use and freshly diluted in complete culture medium to 25, 50, or 100 μg/mL. These working solutions contained no added DMSO or other organic solvent. The pH of the final treatment medium was checked to ensure that preparation had not caused obvious acidification or alkalization. For oral gavage, distilled water was used to adjust the extract to the required crude drug-equivalent concentrations. Although the extract itself was not tested for endotoxin, sterile handling and endotoxin-free consumables were used wherever applicable [8].

2.2. Cell culture

Caco-2 intestinal epithelial cells were obtained from the Shanghai Cell Bank of the Chinese Academy of Sciences (Shanghai, China). Cultures were maintained at 37 °C under humidified 5% CO_2 in DMEM supplemented with fetal bovine serum (10%), penicillin (100 U/mL), and streptomycin (100 μg/mL) [9].

2.3. Cell treatment and grouping

Each well of a 6-well plate received 2×10^5 cells, which were left to adhere overnight at 37 °C in 5% CO_2. Once cultures reached approximately 70–80% confluence, they were randomly allocated to six groups: control, TNF-α model, mesalazine, and low-, medium-, or high-concentration SXS [10]. The model and treatment groups were exposed to tumor necrosis factor-alpha (TNF-α; 10 ng/mL) for 24 h to induce epithelial injury. In the three SXS groups, 25, 50, or 100 μg/mL SXS was added 1 h before TNF-α exposure, respectively. Mesalazine at 100 μg/mL was the reference treatment, and the assigned interventions were maintained throughout the exposure period [11]. Selection of the SXS concentration range was guided by preliminary viability screening and CCK-8 cytotoxicity testing, neither of which indicated obvious cytotoxicity at these concentrations. Accordingly, 25, 50, and 100 μg/mL were designated the low, medium, and high concentrations for the intervention experiments.

The control group was treated with the corresponding vehicle alone, without TNF-α or SXS. After incubation, cell samples and culture supernatants were collected for assessments of viability, cytokines, tight junctions, and protein expression [12].

2.4. Cell viability assay

Cell viability was evaluated by CCK-8 in 96-well plates seeded with 1×10^4 cells per well. On completion of the planned treatments, each well received 10 μL of CCK-8 reagent and was incubated for a further 2 h. Absorbance was then read at 450 nm on a microplate reader, with values normalized to those of the control group.

2.5. Assessment of inflammatory injury in vitro

To quantify the inflammatory response of epithelial cells, culture supernatants were harvested after incubation and assayed for IL-6, IL-1β, and PGE2 by ELISA, following the kit manufacturer's protocol. RNA and protein samples were also collected at the relevant time points for subsequent qPCR and Western blot analyses.

2.6. Barrier function assessment of intestinal epithelium

Two complementary measurements were used to assess epithelial barrier integrity: transepithelial electrical resistance (TEER) and FITC-dextran permeability [13]. For the resistance assay, Caco-2 cells were plated at 1×10^5 cells/well on polycarbonate Transwell inserts with 0.4-μm pores. Monolayers were allowed to differentiate and develop a stable barrier over 21 days, with medium changes every 2 days. TEER was tracked throughout this period, and subsequent experiments included only monolayers whose baseline resistance had stabilized [14]. Mature monolayers had a pretreatment TEER of approximately 650 $\Omega \cdot cm^2$. An EVOM2 epithelial voltohmmeter (World Precision Instruments, USA) was used to record resistance. The reading from a blank insert was subtracted from each sample reading, and the resulting value was multiplied by the membrane area to obtain TEER in $\Omega \cdot cm^2$.

Paracellular tracer flux was assessed by placing 4-kDa FITC-dextran at 1 mg/mL in the upper Transwell chamber. After 2 h at 37 °C, a 100-μL aliquot was carefully collected from the lower chamber. Fluorescence was measured with a microplate reader at 485 nm excitation and 530 nm emission as an indicator of monolayer permeability [15].

2.7. Western blotting experiment

Cell and colorectal tissue proteins were obtained by lysis in RIPA buffer supplemented with protease inhibitors. Equal protein amounts were combined with 5× SDS loading reagent, heated for 5 min at 95 °C, resolved by 10–12% SDS-PAGE, and electrotransferred to PVDF membranes. Membranes

were blocked for 1 h in TBST containing 5% non-fat milk, then incubated at 4 °C overnight with antibodies against ZO-1, occludin, and claudin-1 (1:1000 each) or β-actin (1:5000). The appropriate HRP-conjugated secondary antibodies were applied for 1 h at room temperature. ECL detection was followed by ImageJ densitometry. Total target-protein abundance was normalized to β-actin from the same sample, whereas signaling activation was expressed as the phosphorylated-to-total protein ratio: p-p65/p65, p-IκBα/IκBα, or p-MLC/MLC [16]. Exposure settings were adjusted to prevent saturation, and densitometry was restricted to images acquired within the linear detection range. The supplementary materials contain full-length Western blots with molecular weight markers and representative β-actin loading controls.

2.8. Animals

Male C57BL/6 mice (6–8 weeks old; 20–25 g) were supplied by the Nanjing Laboratory Animal Center in Jiangsu Province. Animals were kept under specific pathogen-free (SPF) conditions at 22 ± 2 °C and 50–60% relative humidity, on a 12-h light–dark cycle. Feed and pure water were freely available throughout the experiment [17]. The study used males only to reduce variability associated with the estrous cycle and fluctuations in sex hormones, both of which may affect inflammation and intestinal barrier function in DSS-induced colitis [18].

Before experiments began, the mice underwent at least 7 days of acclimatization. Procedures followed the "Standards for Care and Use of Laboratory Animals" and were approved by the Animal Welfare Committee of Jiangsu Province Hospital of Chinese and Western Medicine under license HK-20241127-042.

Preliminary concentration-ranging tests, together with CCK-8 viability measurements, informed the choice of SXS concentrations for the cell experiments [19]. Under the conditions tested, viability was not significantly reduced by 25, 50, or 100 μg/mL SXS. These concentrations were therefore assigned as the low, medium, and high working levels, respectively.

All animal doses refer to crude drug equivalents. Previous reports describe an adult daily SXS amount of approximately 20 g of crude herbs. To place the mouse doses in a human context, body surface area normalization was applied as HED (g/kg) = mouse dose (g/kg) × Km_mouse/Km_human, using Km_mouse = 3 and Km_human = 37. For a 60-kg adult, the resulting estimates were approximately 4.9, 9.7, and 19.5 g/day for mouse doses of 1, 2, and 4 g/kg/day, respectively [20]. This calculation provides only an approximate translational comparison; it does not establish clinical dose equivalence or safe doses for humans.

Following one week of acclimatization, mice were randomized into six groups of six animals: control, DSS model, mesalazine, and low-, medium-, or high-dose SXS. The acute colitis protocol comprised 7 consecutive days of drinking water containing 3% dextran sulfate sodium (DSS), followed by 3 days of regular water. The three SXS groups received SXS by oral gavage once daily at 1, 2, or 4 g/kg/day, respectively [21]. These low, medium, and high doses were expressed as crude drug equivalents and chosen with reference to earlier pharmacological work on SXS-related herbal preparations and preliminary tolerability observations. Body surface area conversion yields approximate human-equivalent amounts of 4.9, 9.7, and 19.5 g/day for a 60-kg adult, respectively. General condition, behavior, body weight, and visible signs of adverse effects were checked every day [22].

Mesalazine served as the positive control at 100 mg/kg/day. Treatment began on the first day of DSS exposure and was maintained through the experimental endpoint; the control and DSS model groups were gavaged with the same volume of distilled water [23]. Body weight, stool consistency, and fecal bleeding were recorded daily throughout the 10-day period. Disease activity index (DAI) scores were calculated from body weight loss, stool consistency, and fecal bleeding. On day 10, after the 3 days of regular drinking water, mice were deeply anesthetized with sodium pentobarbital and euthanized by cervical dislocation in accordance with the approved protocol [24]. Blood and colon tissues were collected to assess colon length, histology, inflammatory cytokines, permeability-related markers, and tight junction proteins. Animal work followed the approved institutional care protocol, and reporting referred to the ARRIVE guidelines where applicable.

2.9. Evaluation of clinical manifestations

Clinical monitoring continued daily for all 10 experimental days [25]. Weight records, stool consistency, and the presence of fecal bleeding formed the basis of the DAI assessment. At the endpoint, colon length was recorded and tissue specimens were retained for histological and molecular evaluation.

2.10.Assessment of intestinal permeability and serum barrier injury markers

Circulating evidence of mucosal barrier injury was assessed through serum DAO activity and D-lactate concentration [26]. DAO is predominantly located in mature intestinal epithelial cells and can enter the circulation after mucosal damage. D-lactate, largely a product of intestinal bacterial metabolism, may accumulate in serum when gut permeability increases. The two serum measures were interpreted alongside FITC-dextran permeability and serum LPS to assess barrier dysfunction [27].

For serum LPS analysis, blood was drawn into endotoxin-free tubes and processed under sterile conditions to separate serum. Samples remained at −80 °C until testing, without repeated freeze–thaw cycles [28]. A commercial ELISA kit was used following the supplier's protocol; every assay included a standard curve and blank controls, and each serum sample was tested in duplicate. Separate commercial kits were used to determine DAO activity and D-lactate concentration according to their respective instructions.

2.11.Histopathological examination

Colon specimens underwent fixation in 4% paraformaldehyde for 24 h, followed by graded ethanol dehydration and paraffin embedding. Sections cut to 4 μm were processed with standard hematoxylin and eosin (H&E) staining. Images representing each group were obtained at 40× and 200× with the same acquisition settings [29]. Two investigators independently scored injury while unaware of group assignments. The predefined assessment criteria covered epithelial damage, loss of crypt structure, inflammatory cell infiltration, and mucosal erosion. For each animal, several nonoverlapping fields were randomly chosen from representative sections, and the two investigators' scores were averaged before statistical analysis. Folded sections were excluded from evaluation; damaged tissue margins and

areas with clear staining artifacts were also omitted from scoring [30].

2.12.Randomization and blinding

Random group assignment took place after acclimatization for mice and after the required confluence had been reached for cell cultures [31]. Two independent observers, both unaware of treatment allocation, carried out histological scoring. Where applicable, sample codes were used for image-based measurements, including histological image analysis and Western blot densitometry. Statistical testing followed completion of data collection and decoding of group identities.

2.13.Statistical analysis

Results are reported as mean ± standard deviation (SD). Each animal group contained six mice. This number was chosen with reference to earlier DSS colitis studies and preliminary observations, balancing reduced animal use against the ability to detect differences in major disease outcomes [32]; no formal power calculation was undertaken. Every in vitro assay was repeated in at least three independent biological experiments. Within each experiment, CCK-8 and ELISA used technical replicate wells, while TEER and FITC-dextran permeability used separate Transwell inserts as technical replicates. Independently prepared cell samples were used for qRT-PCR and Western blotting. Data analysis was carried out in GraphPad Prism 9.0 and SPSS 26.0. For comparisons across multiple groups, one-way ANOVA was combined with Tukey's post hoc test. The longitudinal body weight and DAI measurements were evaluated by two-way repeated-measures ANOVA, followed by appropriate post hoc multiple comparisons. Key comparisons were accompanied by exact P values where applicable, and statistical significance was defined as $P < 0.05$.

3. Results

3.1. Shixiaosan improves DSS-induced colitis and damage of colon tissue

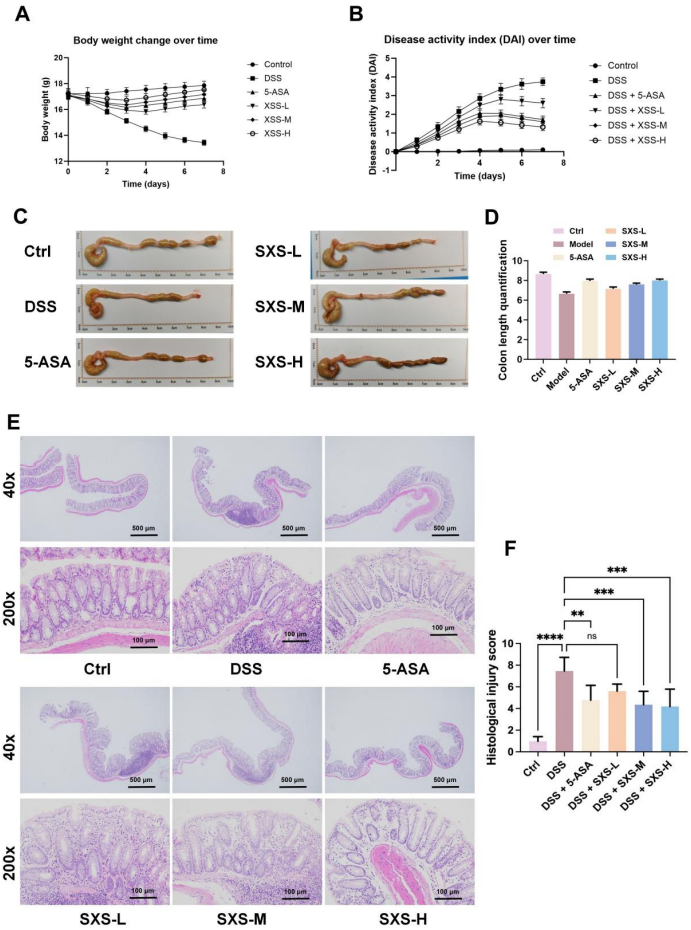


Figure 1. Colitis severity and colonic injury following Shixiaosan treatment in DSS-exposed mice. (A) Body weight trajectories across the 10-day experiment: 7 days of DSS administration and a subsequent 3 days of regular drinking water. (B) DAI scores over the same interval. (C) Representative gross views of the colon in each group. (D) Colon length measurements. (E) Representative colonic H&E images at low and high magnification; upper and lower panels have scale bars of 500 μm and 100 μm, respectively. (F) Histological injury scores. Values are reported as mean ± SD. ns, not significant; **P < 0.01; ***P < 0.001; ****P < 0.0001.

Each group comprised 6 mice, and values are summarized by the mean ± SD. Body weight and DAI trajectories were evaluated using two-way repeated-measures ANOVA with post hoc multiple comparisons. For colon length and histological injury scores, one-way ANOVA was followed by Tukey's post hoc test. Supplementary Table S2 lists exact P values for the key comparisons. Statistical notation: ns, not significant; **P < 0.01; ***P < 0.001; ****P < 0.0001.

The DSS colitis model was used to assess whether Shixiaosan (SXS) could limit inflammatory intestinal injury in vivo. Mice receiving DSS alone progressively lost body weight. This loss was less pronounced with SXS, and the

greatest protection occurred at the high dose, with a response comparable to that of the reference treatment (Figure 1A). Disease activity index (DAI) scores, which combine weight loss, stool changes, and bleeding [33], also rose after DSS exposure. SXS treatment progressively lowered these scores (Figure 1B).

At macroscopic examination, colons from DSS-exposed mice tended to be shorter than those from controls. SXS partly counteracted this change, most visibly in the medium- and high-dose groups (Figure 1C, D). The between-group difference in colon length was modest; accordingly, colon length served as supporting evidence of colitis severity and was interpreted alongside DAI and tissue histology.

Histological examination of H&E-stained sections identified pronounced colonic injury after DSS exposure. Whereas control tissue retained an intact mucosa, orderly crypts, and little inflammatory infiltration, DSS-exposed tissue showed disrupted epithelium, loss of crypts, disorganized mucosal architecture, and prominent infiltrating inflammatory cells [34]. Both 5-ASA and SXS improved these features to different degrees: epithelial continuity increased, crypt architecture was partly restored, and inflammatory infiltration diminished. SXS-treated mice also had lower histological injury scores than the DSS model group, with the clearest improvements at the medium and high doses (Figure 1E, F).

3.2. Shixiaosan improves intestinal barrier dysfunction in DSS-induced colitis

Barrier function in the DSS colitis model was examined using intestinal permeability measurements and circulating markers of mucosal injury. For the permeability assay, serum fluorescence was recorded 4 hours after oral FITC-dextran administration (Figure 2A). DSS-exposed mice had significantly more serum FITC-dextran than controls, consistent with increased intestinal permeability and impaired barrier function. SXS significantly attenuated this increase. The largest reduction occurred in the high-dose group and approached the response to 5-ASA (Figure 2B).

Circulating injury markers showed changes consistent with the permeability assay. DSS increased serum DAO activity, whereas SXS significantly reduced it, with greater protection in the high-dose group (Figure 2C). Serum D-lactic acid also rose after DSS exposure; both the medium and high SXS doses significantly attenuated this elevation (Figure 2D). Increased serum LPS in the DSS group suggested that barrier impairment might permit leakage of luminal endotoxin. The lower LPS levels observed after SXS treatment were consistent with a possible improvement in barrier integrity and reduced permeability-related endotoxin leakage (Figure 2E).

Together, the permeability assay and serum-marker findings indicate that SXS limits the intestinal hyperpermeability and mucosal barrier injury caused by DSS, helping to preserve barrier function during inflammation.

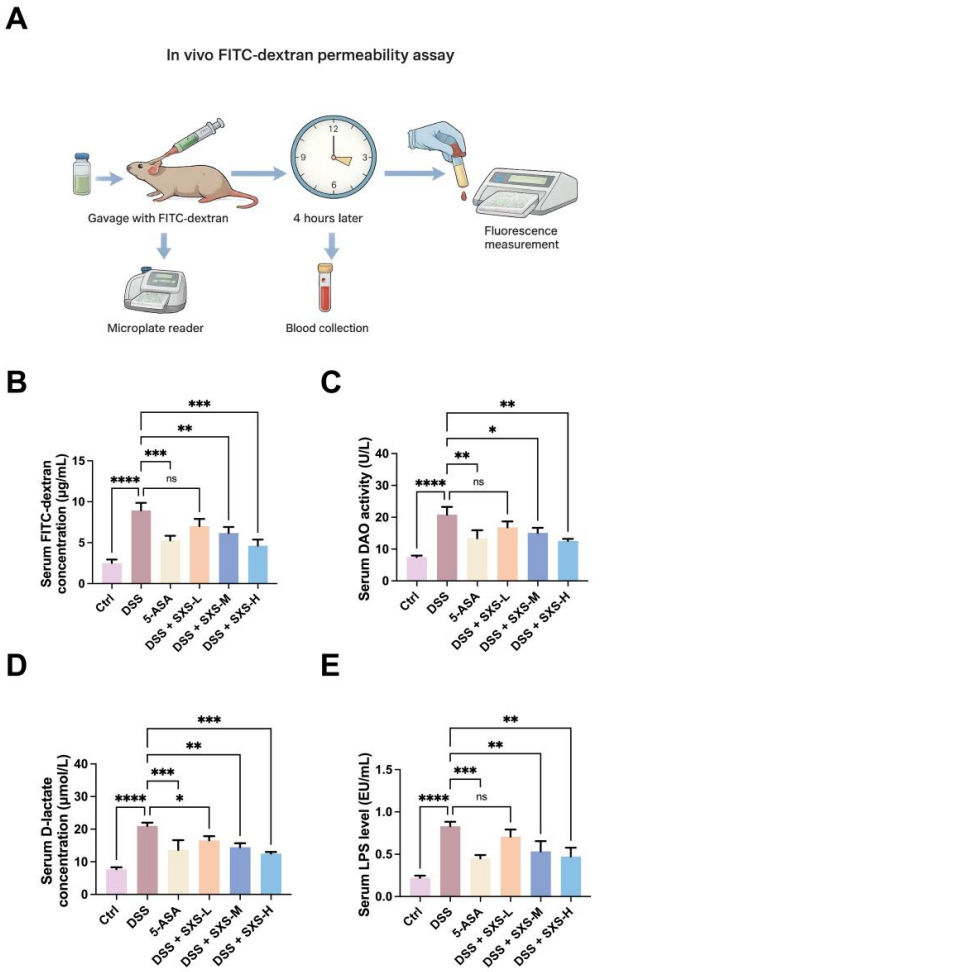


Figure 2. Intestinal permeability and circulating barrier-injury markers in DSS colitis mice treated with Shixiaosan. (A) Overview of the in vivo FITC-dextran permeability assay. The experimental groups are compared for (B) serum FITC-dextran, (C) serum DAO activity, (D) serum D-lactate concentration, and (E) serum LPS.

Values are summarized as mean ± SD. Animal groups contained 6 mice each; cell data, where applicable, came from 3 independent biological experiments. Group comparisons used one-way ANOVA and Tukey's post hoc test. The exact P values for key comparisons are listed in Supplementary Table S2. Significance symbols denote ns, not significant; *P < 0.05; **P < 0.01; ***P < 0.001; ****P < 0.0001.

3.3. Shixiaosan restored expression of tight junction proteins in colon tissue of DSS-induced colitis mice

To investigate whether recovery of tight junctions accompanied the effect of SXS on the barrier, key junctional components were quantified in colonic tissue [35]. DSS significantly lowered ZO-1, occludin, and claudin-1 mRNA abundance relative to controls in the qRT-PCR assay, consistent with impaired epithelial barrier integrity. SXS counteracted these reductions to varying degrees, and recovery was more apparent at the medium and high doses (Figure 3A-C).

The protein measurements likewise showed markedly lower ZO-1, occludin, and claudin-1 levels after DSS exposure than in controls. SXS increased all three proteins; the greatest recovery occurred with the high dose, and the overall response resembled that to 5-ASA (Figure 3D-G). Thus, loss of junctional proteins accompanied DSS-induced colonic barrier injury, while restoration of their expression by SXS was consistent with preservation of epithelial integrity [36].

Taken together, these observations indicate that SXS helps maintain intestinal mucosal integrity during inflammatory injury by mitigating the increases in permeability and epithelial barrier damage associated with DSS.

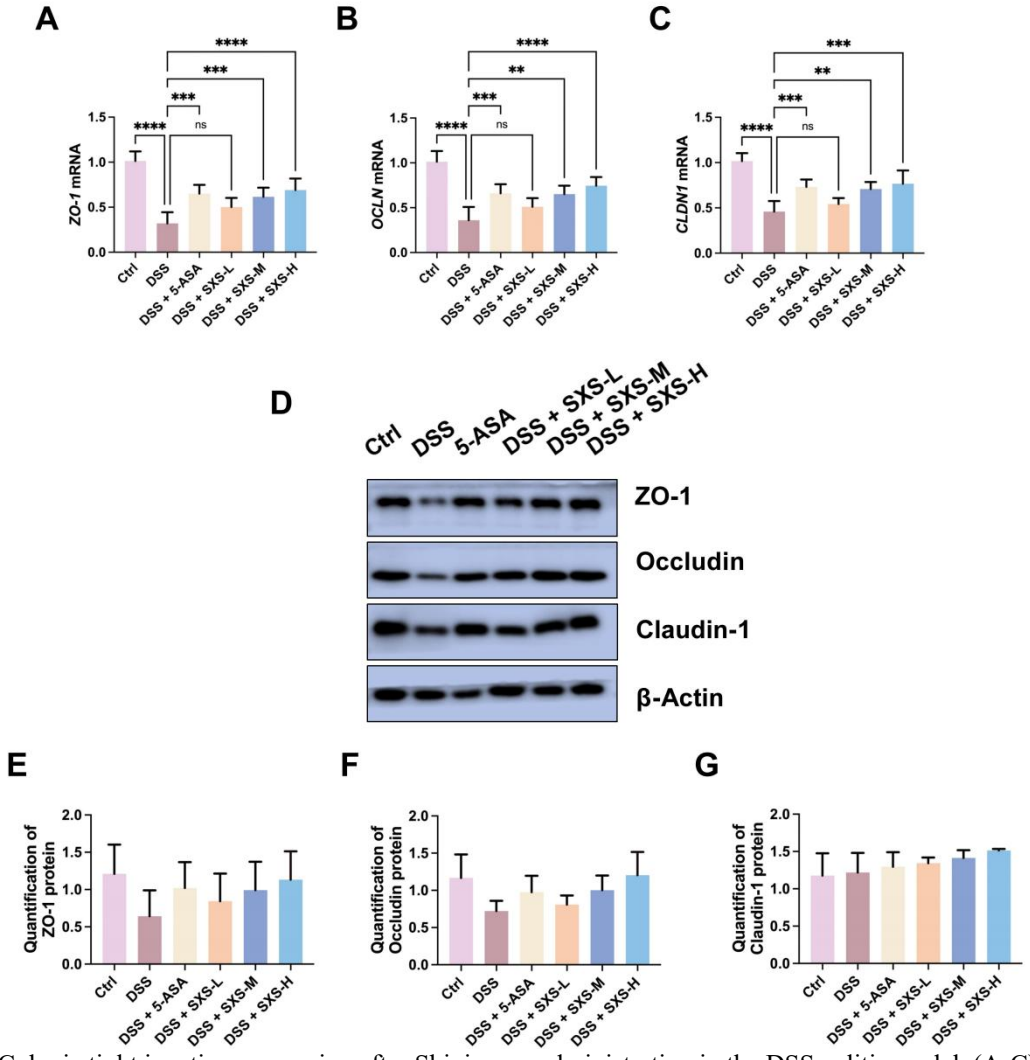


Figure 3. Colonic tight junction expression after Shixiaosan administration in the DSS colitis model. (A-C) qRT-PCR measurements of relative ZO-1, occludin, and claudin-1 mRNA abundance. (D) Representative immunoblots of these three proteins across the experimental groups. (E-G) Protein quantification relative to the internal control. Values are mean ± SD. *P < 0.05; **P < 0.01; ***P < 0.001; ****P < 0.0001.

Results are reported as mean ± SD, with 6 mice in each animal group and, where applicable, 3 independent biological experiments for cell assays. One-way ANOVA with Tukey's post hoc test was used for statistical comparisons. Key comparisons and their exact P values appear in Supplementary Table S2. ns denotes no significant difference; *P < 0.05; **P < 0.01; ***P < 0.001; ****P < 0.0001.

3.4. Shixiaosan protects intestinal epithelial cells from TNF-α-induced barrier dysfunction (in vitro experiment)

A TNF-α-induced epithelial injury model was used to

examine the direct effects of SXS on the barrier under inflammatory conditions. Initial CCK-8 screening detected no cytotoxicity from SXS at any concentration tested (Figure 4A). TNF-α significantly decreased cell viability, and both 5-ASA and SXS partly opposed this decrease. Recovery was greater in the medium- and high-concentration SXS groups (Figure 4B).

Electrical resistance and tracer flux provided complementary measures of monolayer barrier function. TEER remained stable in untreated cells but declined progressively after TNF-α exposure, indicating loss of barrier integrity. SXS limited this decline in a concentration-dependent manner; the highest concentration produced the greatest protection, approaching that achieved with 5-ASA (Figure 4C, D). TNF-α also increased FITC-dextran passage across the monolayer. This increase was effectively inhibited by the medium and high SXS concentrations (Figure 4E).

TNF-α significantly lowered ZO-1, OCLN, and CLDN1 mRNA levels, with SXS producing a partial recovery of these transcripts (Figure 4F-H). The barrier stability index also tended to recover after treatment, although the differences among treatment groups did not reach statistical significance (Figure 4I). These in vitro findings support a direct protective effect of SXS on intestinal mucosal cells and attenuation of permeability-related injury [37].

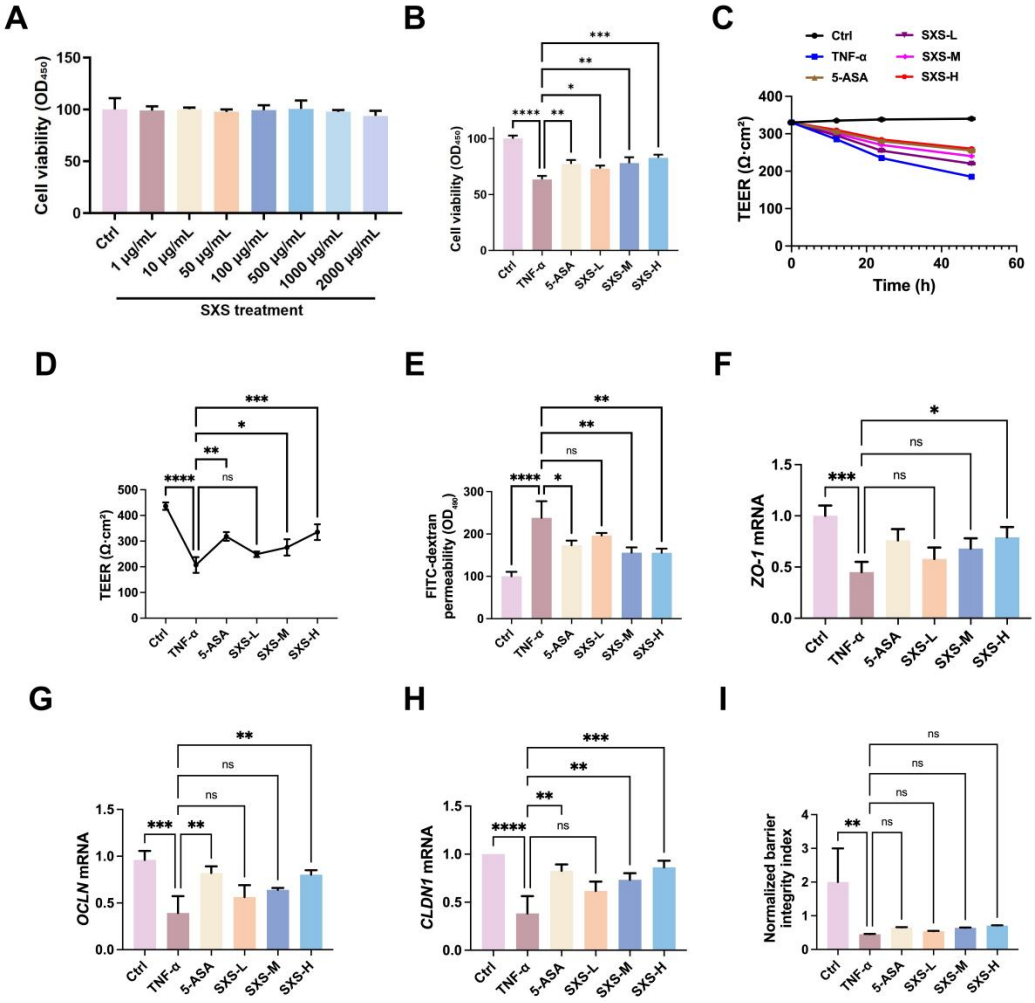


Figure 4. Functional and transcriptional measures of the epithelial barrier following TNF-α exposure and Shixiaosan intervention. (A) Cell viability across the tested SXS concentrations. (B) Viability in the control, TNF-α, 5-ASA, and SXS experimental groups after TNF-α stimulation. TEER is shown as (C) a time course and (D) endpoint measurements. (E) FITC-dextran transport through epithelial monolayers. (F–H) Relative transcript levels of ZO-1, OCLN, and CLDN1 following TNF-α stimulation and SXS treatment. (I) Barrier integrity index after normalization. Values are mean ± SD. ns, not significant; *P < 0.05; **P < 0.01; ***P < 0.001; ****P < 0.0001.

Values summarize three independent biological experiments as mean ± SD. Two-way repeated-measures ANOVA with post hoc multiple comparisons was used for the TEER time course. Endpoint measurements, including viability, FITC-dextran permeability, qRT-PCR, and the barrier integrity index, were compared using one-way ANOVA followed by Tukey's post hoc test. Supplementary Table S2 provides the exact P values for key comparisons. The notation is ns, not significant; *P < 0.05; **P < 0.01; ***P < 0.001; ****P < 0.0001.

3.5. Shixiaosan suppresses inflammatory responses in DSS-induced colitis and TNF-α-stimulated epithelial cells.

Inflammatory readouts from both models were examined to establish whether reduced inflammation accompanied the preservation of barrier function by SXS. In the colon, DSS markedly increased IL-6, IL-1β, TNF-α, and MPO activity relative to controls, consistent with intestinal inflammation

and inflammatory cell infiltration. SXS lowered these indices to different extents, with more pronounced responses at the medium and high doses. The high-dose group, in particular, had lower MPO activity than the DSS model group, supporting attenuation of colonic inflammatory infiltration (Figure 5A–D).

The cell model showed a corresponding inflammatory response: TNF-α significantly elevated IL-6, IL-1β, and PGE2 levels in intestinal epithelial cells. SXS curtailed production of these mediators, with the clearest reductions at the medium and high concentrations. These changes indicate attenuation of the TNF-α-induced inflammatory response in vitro (Figure 5E–G).

Immunoblotting provided an additional assessment of the epithelial inflammatory response. COX-2 and iNOS expression was higher after TNF-α stimulation than in control cells (Figure 5H and I), in agreement with the ELISA measurements of inflammatory mediators. Both proteins were reduced by 5-ASA or SXS to varying degrees, and inhibition was more evident in the medium- and high-concentration SXS groups. Considered together with the animal findings, these results support an anti-inflammatory effect of SXS in DSS colitis and in TNF-α-exposed epithelial cells.

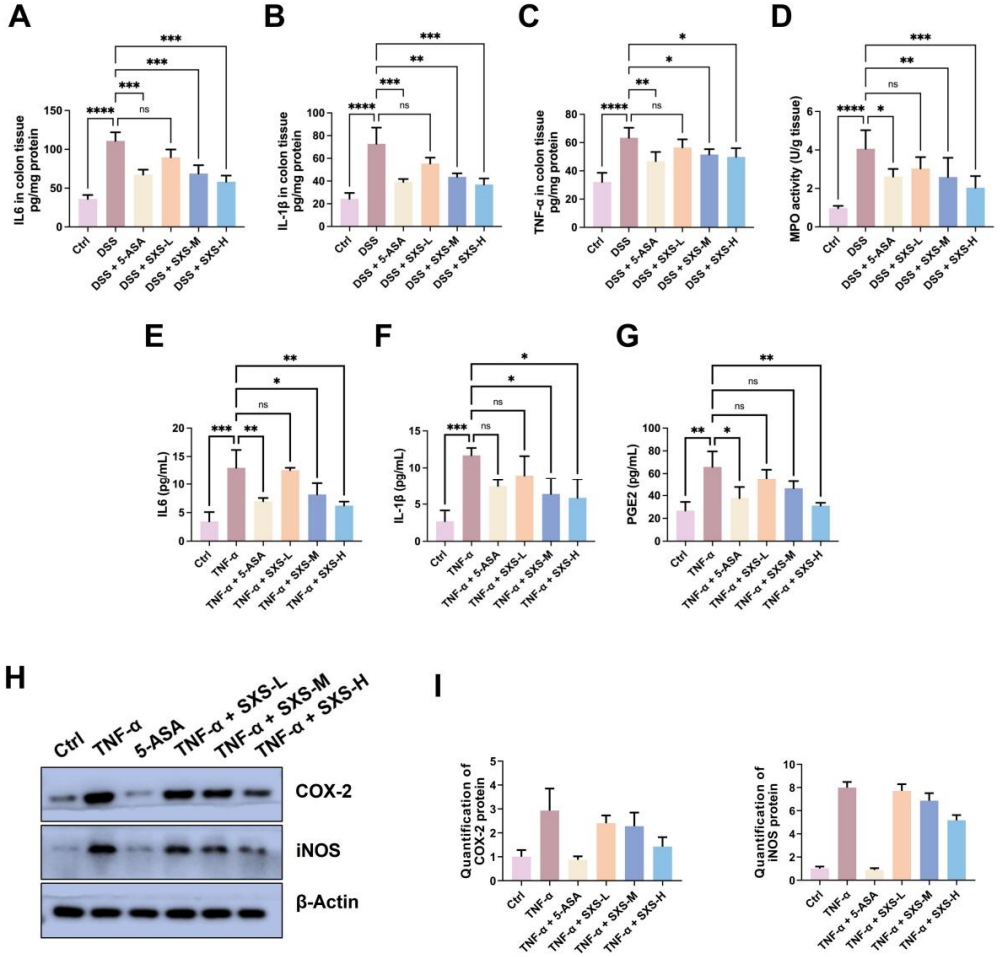


Figure 5. Inflammatory markers in DSS colitis mice and TNF-α-exposed epithelial cells following Shixiaosan treatment. (A–D) Colonic IL-6, IL-1β, TNF-α, and MPO activity across the experimental groups. (E–G) Epithelial IL-6, IL-1β, and PGE2 levels following TNF-α stimulation and SXS intervention. (H) Representative COX-2 and iNOS immunoblots from epithelial cells. (I) COX-2 and iNOS protein quantification relative to β-actin. Values are mean ± SD. ns, not significant; *P < 0.05; **P < 0.01; ***P < 0.001; ****P < 0.0001.

Data are summarized by the mean ± SD. Sample sizes were 6 mice per animal group and 3 independent biological experiments for the applicable cell assays. One-way ANOVA with Tukey's post hoc test was used to compare groups, with exact P values for key comparisons reported in Supplementary Table S2. Symbols indicate ns, not significant; *P < 0.05; **P < 0.01; ***P < 0.001; ****P < 0.0001.

3.6. RELA silencing supports the involvement of NF-κB-associated MLC phosphorylation in the barrier-protective effects of Shixiaosan

SXS-M consistently showed protective responses across the viability, TEER, permeability, inflammatory mediator, and tight junction assays. It was therefore chosen as the representative concentration for the subsequent signaling analyses and RELA-knockdown experiments.

NF-κB activation and MLC phosphorylation were evaluated in the TNF-α cell model to relate signaling responses to the observed barrier protection. Relative to controls, TNF-α markedly elevated the p-p65/p65, p-IκBα/IκBα, and p-MLC/MLC ratios (Figure 6A and B). SXS-M reduced these elevations, while treatment with SXS-M alone caused little change in basal protein levels. TNF-α also lowered ZO-1, occludin, and claudin-1 expression. These junctional proteins recovered to varying extents after 5-ASA or SXS treatment, with more apparent recovery in the SXS-

M and SXS-H groups (Figure 6C).

Three RELA-targeting siRNAs were compared to test the functional contribution of NF-κB signaling. Each construct lowered p65 protein expression relative to siNC; siRELA-3 achieved the strongest knockdown and was used in the remaining experiments (Figure 6D). In TNF-α-stimulated cells, RELA knockdown reduced the p-MLC signal and partly restored ZO-1, occludin, and claudin-1 compared with TNF-α-treated siNC cells (Figure 6E and F). With SXS-M treatment, junctional protein recovery in RELA-silenced cells was maintained or further improved.

The knockdown findings functionally implicate RELA/NF-κB signaling in the MLC phosphorylation and tight junction disruption triggered by TNF-α. Nevertheless, MLCK was neither directly measured nor genetically manipulated, and rescue experiments were not performed. The data therefore do not establish a fully linear causal sequence from RELA through MLCK to tight junctions, nor do they show that SXS protection depends exclusively on RELA.

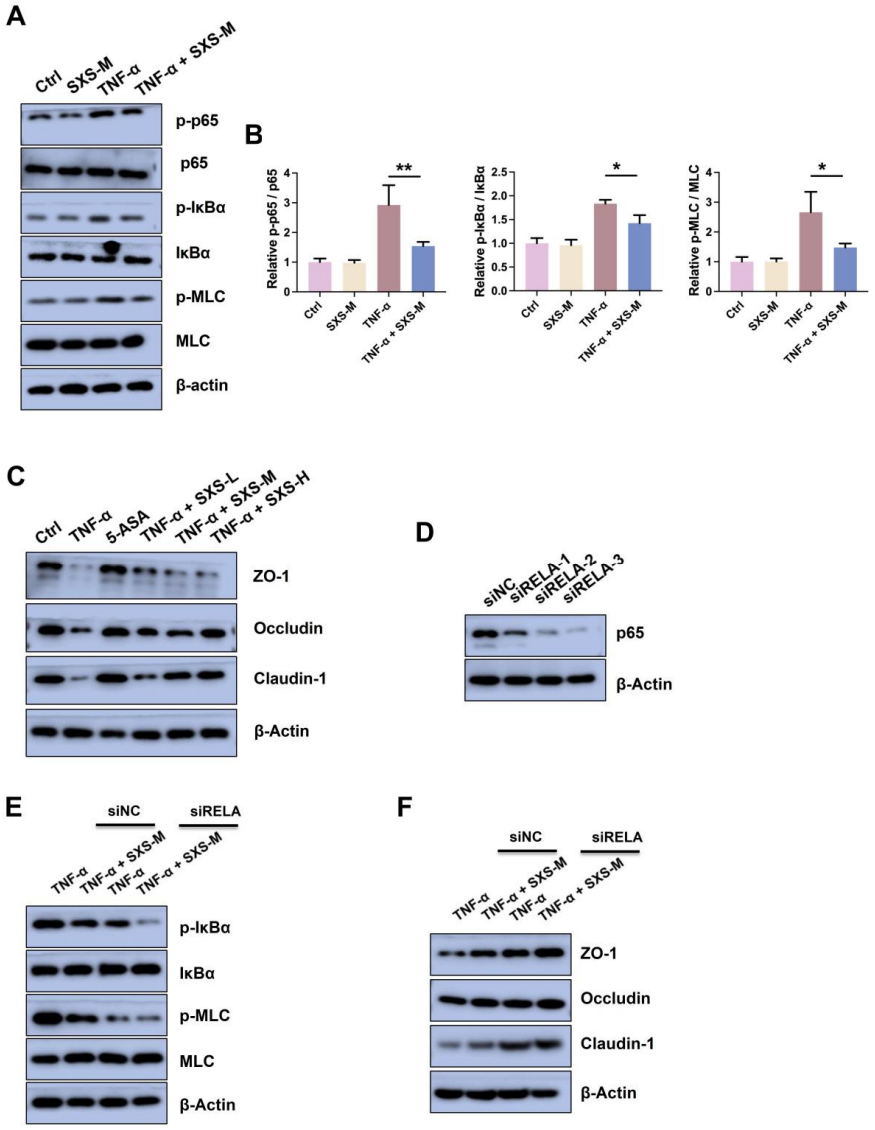


Figure 6. NF-κB signaling, MLC phosphorylation, and junctional proteins after Shixiaosan treatment, assessed alongside RELA silencing. (A) Representative immunoblots of p-p65, p65, p-IκBα, IκBα, p-MLC, MLC, and β-actin from control, SXS-M, TNF-α, and TNF-α + SXS-M cells. (B) Quantified ratios of p-p65 to p65, p-IκBα to IκBα, and p-MLC to MLC. (C) Representative ZO-1, occludin, claudin-1, and β-actin immunoblots for the control, TNF-α, TNF-α + 5-ASA, TNF-α + SXS-L, TNF-α + SXS-M, and TNF-α + SXS-H groups. (D) Representative p65 immunoblots from Caco-2 cells receiving siNC, siRELA-1, siRELA-2, or siRELA-3; siRELA-3 was used for subsequent experiments. (E) Representative immunoblots of p-IκBα, IκBα, p-MLC, MLC, and β-actin in TNF-α-exposed cells transfected with siNC or siRELA, with or without SXS-M. (F) Representative ZO-1, occludin, claudin-1, and β-actin immunoblots from the corresponding siNC and siRELA groups. SXS-L, SXS-M, and SXS-H denote concentrations of 25, 50, and 100 μg/mL, respectively. Panel B summarizes three independent biological experiments as mean ± SD; comparisons used one-way ANOVA followed by Tukey's post hoc test. *P < 0.05; **P < 0.01.

4. Discussion

SXS improved several measures of intestinal epithelial injury in the mouse and cell models examined here. In DSS-treated mice, treatment limited body weight loss and DAI elevation, improved tissue architecture, and partly counteracted colon shortening. These changes occurred alongside lower circulating FITC-dextran, DAO, D-lactate,

and LPS and recovery of colonic ZO-1, occludin, and claudin-1. The relatively small difference in colon length warrants caution: this macroscopic measure provides supportive evidence when considered with DAI, histology, inflammatory mediators, permeability measures, and junctional protein expression, but does not independently establish disease severity. In Caco-2 cells, the tested SXS concentrations showed no obvious cytotoxicity. SXS counteracted TNF-α-associated reductions in viability and TEER, limited FITC-dextran passage, and restored tight-junction-related proteins. The agreement between these observations supports a role for SXS in preserving epithelial barrier integrity under the experimental inflammatory conditions.

Greater intestinal permeability facilitates the passage of luminal antigens, microbial metabolites, and endotoxin into mucosal tissues and is commonly associated with inflammatory bowel disease. In this study, SXS-treated DSS mice showed lower circulating FITC-dextran together with lower DAO, D-lactate, and LPS. The cell experiments provided complementary functional evidence, as SXS limited the TNF-α-induced fall in TEER and the increase in FITC-dextran flux. This pattern suggests an effect on the epithelial barrier itself in addition to a reduction in systemic inflammation. The serum biomarkers nevertheless require qualified interpretation. DAO is concentrated in mature intestinal epithelial cells, and increased circulating activity can accompany epithelial injury. D-lactate originates largely from bacterial metabolism, so its accumulation in blood may reflect greater permeability to microbial metabolites. Neither measurement directly quantifies barrier function, and both can be influenced by epithelial turnover, systemic metabolism, sample handling, and assay conditions. Accordingly, DAO and D-lactate were considered alongside tracer permeability, serum LPS, histological damage, and tight-junction protein expression.

Junctional integrity also depends on proteins such as ZO-1, occludin, and claudin-1, whose abundance or localization can change during inflammatory injury. Their reduction in DSS-exposed colonic tissue and TNF-α-treated epithelial cells was attenuated by SXS, consistent with improved junctional stability in both models. This is relevant because inflammation and barrier disruption can reinforce one another: TNF-α can damage epithelial cells and weaken tight junctions, while greater paracellular passage can further intensify mucosal inflammation. DSS increased colonic IL-6, IL-1β, TNF-α, and MPO activity, and TNF-α stimulation increased IL-6, IL-1β, and PGE2 in the cell model. SXS reduced these inflammatory readouts in both settings. The lower MPO activity was also consistent with less inflammatory cell infiltration in the colon. Thus, preservation of junctional components and attenuation of the inflammatory environment may both contribute to the barrier protection observed with SXS.

The signaling experiments provide additional insight into these effects. TNF-α increased the ratios of p-p65/p65, p-IκBα/IκBα, and p-MLC/MLC, and SXS-M limited each increase. RELA knockdown likewise reduced TNF-α-associated MLC phosphorylation and partly recovered ZO-1, occludin, and claudin-1. This gene-silencing evidence supports a functional contribution of RELA/NF-κB to MLC phosphorylation and junctional disruption, beyond the associations seen in phosphorylation measurements alone. Protection was still observed when SXS-M was combined with RELA silencing, however, suggesting that other routes may contribute to the response. Because MLCK was neither measured directly nor experimentally manipulated, these findings cannot establish a complete causal sequence from RELA through MLCK to tight-junction injury.

The observed signaling changes leave several parts of the proposed mechanism unresolved. Although the results suggest modulation of NF-κB/MLCK-related signaling by SXS, the experiments did not systematically address upstream receptors or downstream transcriptional regulation. TNF receptor signaling may be relevant in the TNF-α-stimulated cell model, whereas microbial products and pattern-recognition receptors may contribute to inflammatory amplification in DSS-treated mice. Only a selected set of inflammatory mediators and proteins was measured. Analyses of p65 nuclear localization, NF-κB transcriptional activity, receptor activation, and a wider range of NF-κB target genes are needed to define the signaling network more fully.

Additional mechanisms could influence the response to SXS. Oxidative stress can accompany epithelial injury and junctional disruption, raising the possibility that antioxidant effects contribute to protection. Microbial dysbiosis and the movement of microbial metabolites are also relevant to DSS colitis. Epithelial repair further depends on the balance between apoptosis and proliferation, while recruitment of immune cells to the lamina propria can amplify inflammation. None of these processes was directly examined here. Future work could assess oxidative stress by ROS detection, apoptosis by TUNEL staining, proliferation by Ki-67 staining, lamina propria immune populations by flow cytometry, and microbial composition by 16S rRNA sequencing.

A strength of this study is the use of both a mouse colitis model and an epithelial cell model, assessed through clinical signs, histology, permeability, circulating barrier-related markers, junctional proteins, inflammatory mediators, and signaling readouts. Several limitations constrain interpretation. First, the RELA-silencing experiments support NF-κB involvement but do not resolve the entire mechanism. MLCK knockdown or overexpression, RELA rescue, pathway-specific pharmacological interventions, and direct assessments of NF-κB nuclear translocation or transcriptional activity were not performed. Moreover, part of the pathway analysis used only SXS-M. Its selection reflected consistent protection in the functional assays, but signaling responses at all three SXS levels remain to be compared. Second, chemical characterization was incomplete. Commercial reference standards supported preliminary confirmation of representative constituents, but comprehensive HPLC–Q-TOF–MS profiling, marker quantification, and assessment of consistency between batches were not undertaken. Chromatographic fingerprints, MS/MS-based identification, and quantitative measurement of major constituents should be incorporated into future quality control. Third, DAO and D-lactate provide indirect evidence and are susceptible to biological and analytical influences; their interpretation therefore depends on the accompanying tracer, LPS, histological, and junctional protein findings. The serum LPS assay included a standard curve and blanks, but spike-recovery validation and direct testing of the extract for endotoxin were not performed, leaving potential endotoxin-related interference unresolved. The contribution of yellow rice wine-derived components was not isolated either. Although the extract was concentrated and vehicle controls were included, a control extract prepared through the same wine-based procedure is needed to assess solvent-related

effects more directly. Generalizability is also limited by the exclusive use of male mice to reduce hormone-related variability. Animal numbers were based on earlier DSS studies and preliminary observations rather than a formal power calculation. Follow-up studies should include female mice, prospective power analysis, and larger samples, together with microbiota analysis, ROS measurements, TUNEL and Ki-67 staining, and flow cytometry of lamina propria immune cells to examine epithelial repair and immune responses. Finally, daily observation revealed no obvious mortality, abnormal behavior, or severe systemic adverse signs in the high-dose group, but food and water intake were not quantified. Organ toxicity, long-term safety, and pharmacokinetics were not evaluated. Detailed toxicity testing, intake monitoring, organ function assessment, and pharmacokinetic studies are therefore required before the safety margin, exposure characteristics, or translational relevance of the tested doses can be defined.

5. Conclusion

SXS reduced inflammatory intestinal injury and helped preserve the epithelial barrier, with recovery of tight-junction-related proteins and attenuation of inflammatory responses. RELA silencing reproduced part of the observed response in MLC phosphorylation and junctional protein expression, supporting the involvement of NF-κB signaling. The causal sequence remains unresolved and requires MLCK-specific interventions and rescue experiments. These experimental findings support further investigation of SXS for intestinal inflammatory conditions involving epithelial barrier dysfunction.

Declarations

Ethics approval and consent to participate

Approval for the animal experiments was granted by the Animal Ethics Committee of Jiangsu Province Hospital of Chinese and Western Medicine (HK-20241127-042). The work followed institutional requirements for laboratory animal care and use, with reporting guided by ARRIVE where applicable.

Consent for publication

This manuscript presents original work that has not appeared previously in any language or format and is not being considered for publication elsewhere. As it contains no identifiable personal data or images, individual consent for publication was not required.

Data Availability Statement

Data generated or analyzed in this study may be obtained from the corresponding author upon reasonable request.

Conflicts of Interest

The authors declare no conflict of interest.

Funding

This work received no specific funding.

Authors' contributions

Tianyu She and Bei Huang developed the study concept and experimental design. Experiments and data collection were carried out by Tianyu She, Bei Huang, Yunlong Gao, Weiling Liu, Wenjing Yan, and Qiyi Hu. Xiaoying Tian, Xiaoxiao Zhao, Yina Zhao, Hangyan Qian, Na Jing, and Yuan Wang undertook data analysis, validation, and interpretation. Dan Yun and Tianyu She provided supervision and critical manuscript revision. Tianyu She prepared the initial draft, and Tianyu She and Bei Huang contributed equally. Review and approval of this revised manuscript by all authors are required before submission. ChatGPT (OpenAI) assisted with English-language revision, including sentence and paragraph rephrasing and reorganization. All AI-assisted revisions require the authors' review and approval before submission. The tool was not used to generate scientific hypotheses, experimental data, figures, statistical analyses, references, or conclusions.

Acknowledgements

Not applicable.

List of Abbreviations

5-ASA, 5-aminosalicylic acid; DAI, disease activity index; DAO, diamine oxidase; DSS, dextran sulfate sodium; ELISA, enzyme-linked immunosorbent assay; FITC, fluorescein isothiocyanate; MLC, myosin light chain; MLCK, myosin light chain kinase; MPO, myeloperoxidase; NF-κB, nuclear factor kappa-light-chain-enhancer of activated B cells; RELA, RELA proto-oncogene, NF-κB subunit (p65); SXS, Shixiaosan; TEER, transepithelial electrical resistance; TNF-α, tumor necrosis factor-alpha.

References

[1] Ahmad, R., Sorrell, M. F., Batra, S. K., Dhawan, P., & Singh, A. B. (2017). Gut permeability and mucosal inflammation: Bad, good or context dependent. Mucosal Immunology, 10(2), 307–317. https://doi.org/10.1038/mi.2016.88.

[2] An, J.-H., Li, Q., Bhang, D.-H., Song, W.-J., & Youn, H.-Y. (2020). TNF-α and INF-γ primed canine stem cell-derived extracellular vesicles alleviate experimental murine colitis. Scientific Reports, 10(1), 2115. https://doi.org/10.1038/s41598-020-59051-4

[3] Awad, W. A., Hess, C., & Hess, M. (2017). Enteric pathogens and their toxin-induced disruption of the intestinal barrier through alteration of tight junctions in chickens. Toxins, 9(2), 60. https://doi.org/10.3390/toxins9020060

[4] Barbara, G., Barbaro, M. R., Fuschi, D., Palombo, M., Falangone, F., Cremon, C., Marasco, G., & Stanghellini, V. (2021). Inflammatory and microbiota-related regulation of the intestinal epithelial barrier. Frontiers in Nutrition, 8, 718356. https://doi.org/10.3389/fnut.2021.718356

[5] Breugelmans, T., De Man, J., De Winter, B., & Smet, A. (2019). P097 Intestinal barrier dysfunction in association with fibrosis during experimental acute and chronic colitis in mice. Journal of Crohn's and Colitis, 13(Suppl. 1), S134–S136. https://doi.org/10.1093/ecco-jcc/jjy222.214

[6] Capaldo, C. T., Powell, D. N., & Kalman, D. (2017). Layered defense: How mucus and tight junctions seal the intestinal barrier. Journal of Molecular Medicine, 95(9), 927–934. https://doi.org/10.1007/s00109-017-1557-x

[7] Chen, C., Tao, T., Wen, C., He, W.-Q., Qiao, Y.-N., Gao, Y.-Q., Chen, X., Wang, P., Chen, C.-P., Zhao, W., Chen, H.-Q., Ye, A.-P., Peng, Y.-J., & Zhu, M.-S. (2014). Myosin light chain kinase (MLCK) regulates cell migration in a myosin regulatory light chain phosphorylation-independent mechanism. Journal

of Biological Chemistry, 289(41), 28478–28488. https://doi.org/10.1074/jbc.M114.574435

[8] Chen, S., Zhang, Y., Niu, X., Mohyuddin, S. G., Wen, J., Bao, M., Yu, T., Wu, L., Hu, C., Yong, Y., Liu, X., Abd El-Aty, A. M., & Ju, X. (2021). Coral-derived endophytic fungal product, butyrolactone-I, alleviates LPS induced intestinal epithelial cell inflammatory response through TLR4/NF-κB and MAPK signaling pathways: An in vitro and in vivo studies. Frontiers in Nutrition, 8, 748118. https://doi.org/10.3389/fnut.2021.748118

[9] Lyu, S.-C., Zhong, G.-Q., Shi, R.-J., Sun, Y., Li, J., Li, M.-S., & Chen, Y. (2025). Diamine oxidase as a biomarker for depression and disease activity in inflammatory bowel disease: A cross-sectional observational study. World Journal of Psychiatry, 15(8), 106971. https://doi.org/10.5498/wjp.v15.i8.106971

[10] Chen, Y., Li, X., Sun, R., Yang, F., Tian, W., & Huang, Q. (2024). Screening and experimental validation of diagnostic gene in ulcerative colitis with anti-TNF-α therapy. IUBMB Life, 76(7), 451–463. https://doi.org/10.1002/iub.2867

[11] Dmytriv, T. R., Storey, K. B., & Lushchak, V. I. (2024). Intestinal barrier permeability: The influence of gut microbiota, nutrition, and exercise. Frontiers in Physiology, 15, 1380713. https://doi.org/10.3389/fphys.2024.1380713

[12] Engevik, A. C., Krystofiak, E. S., Kaji, I., Meyer, A. R., Weis, V. G., Goldstein, A., Coutts, A. W., Melkamu, T., Saqui-Salces, M., & Goldenring, J. R. (2021). Recruitment of polarity complexes and tight junction proteins to the site of apical bulk endocytosis. Cellular and Molecular Gastroenterology and Hepatology, 12(1), 59–80. https://doi.org/10.1016/j.jcmgh.2021.02.007

[13] Feng, Z., Wei, Y., Zhang, Z., Li, M., Gu, R., Lu, L., Liu, W., & Qin, H. (2024). Wheat peptides inhibit the activation of MAPK and NF-κB inflammatory pathways and maintain epithelial barrier integrity in NSAID-induced intestinal epithelial injury. Food & Function, 15(2), 823–837. https://doi.org/10.1039/D3FO02942A

[14] Ficek, J., Wyskida, K., Ficek, R., Wajda, J., Klein, D., Witkowicz, J., Rotkegel, S., Spiechowicz-Zatoń, U., Kocemba-Dyczek, J., Ciepał, J., Więcek, A., Olszanecka-Glinianowicz, M., & Chudek, J. (2017). Relationship between plasma levels of zonulin, bacterial lipopolysaccharides, D-lactate and markers of inflammation in haemodialysis patients. International Urology and Nephrology, 49(4), 717–725. https://doi.org/10.1007/s11255-017-1530-8

[15] Fu, R., Wang, L., Meng, Y., Xue, W., Liang, J., Peng, Z., Meng, J., & Zhang, M. (2022). Apigenin remodels the gut microbiota to ameliorate ulcerative colitis. Frontiers in Nutrition, 9, 1062961. https://doi.org/10.3389/fnut.2022.1062961

[16] Han, J., Li, J.-H., Bai, G., Shen, G.-S., Chen, J., Liu, J.-N., Wang, S., & Liu, X.-J. (2017). Acanthopanax senticosus polysaccharides-induced intestinal tight junction injury alleviation via inhibition of NF-κB/MLCK pathway in a mouse endotoxemia model. World Journal of Gastroenterology, 23(12), 2175–2184. https://doi.org/10.3748/wjg.v23.i12.2175

[17] Iyer, N., & Corr, S. C. (2021). Gut microbial metabolite-mediated regulation of the intestinal barrier in the pathogenesis of inflammatory bowel disease. Nutrients, 13(12), 4259. https://doi.org/10.3390/nu13124259

[18] Kang, J., Zhou, Y., Zhu, C., Ren, T., Zhang, Y., Xiao, L., & Fang, B. (2022). Ginsenoside Rg1 mitigates porcine intestinal tight junction disruptions induced by LPS through the p38 MAPK/NLRP3 inflammasome pathway. Toxics, 10(6), 285. https://doi.org/10.3390/toxics10060285

[19] Li, L., Huang, J., Feng, L., Xu, L., Lin, H., Liu, K., Li, X., & Wang, R. (2024). Altechromone A ameliorates inflammatory bowel disease by inhibiting NF-κB and NLRP3 pathways. Marine Drugs, 22(9), 410. https://doi.org/10.3390/md22090410

[20] Liu, Z., Jiang, J., Yang, Q., Xiong, Y., Zou, D., Yang, C., Xu, J., & Zhan, H. (2016). MicroRNA-682-mediated downregulation of PTEN in intestinal epithelial cells ameliorates intestinal ischemia–reperfusion injury. Cell Death & Disease, 7(4), e2210. https://doi.org/10.1038/cddis.2016.115

[21] Luo, Y., Yu, X., Zhao, P., Huang, J., & Huang, X. (2022). Effects of resveratrol on tight junction proteins and the Notch1 pathway in an HT-29 cell model of inflammation induced by lipopolysaccharide. Inflammation, 45(6), 2449–2464. https://doi.org/10.1007/s10753-022-01684-3

[22] Macura, B., Kiecka, A., & Szczepanik, M. (2024). Intestinal permeability disturbances: Causes, diseases and therapy. Clinical and Experimental Medicine, 24(1), 232. https://doi.org/10.1007/s10238-024-01446-7

[23] Morovic, P., Gonzalez Moreno, M., Trampuz, A., & Karbysheva, S. (2024). In vitro evaluation of microbial D- and L-lactate production as biomarkers of infection. Frontiers in Microbiology, 15, 1406350. https://doi.org/10.3389/fmicb.2024.1406350

[24] Nwako, J., Riedman, A. M., Singh, S., Edwards, K., & McCauley, H. (2025). Enteroendocrine cells regulate barrier integrity and protect against DSS-induced outcomes. Inflammatory Bowel Diseases, 31(Suppl. 1), S46. https://doi.org/10.1093/ibd/izae299.094

[25] Okumura, R., & Takeda, K. (2025). The role of the mucosal barrier system in maintaining gut symbiosis to prevent intestinal inflammation. Seminars in Immunopathology, 47(1), 2. https://doi.org/10.1007/s00281-024-01062-0

[26] Olaru-Stavila, C., Steinmann, S. M., Mester, P., Müller, M., Tcaciuc, E., & Gülow, K. (2026). The gastrointestinal barrier—Mechanisms of barrier dysfunction in liver cirrhosis and spontaneous bacterial peritonitis. Biomedicines, 14(5), 1084. https://doi.org/10.3390/biomedicines14051084

[27] Sánchez-Alcoholado, L., Ordóñez, R., Otero, A., Plaza-Andrade, I., Laborda-Illanes, A., Medina, J. A., Ramos-Molina, B., Gómez-Millán, J., & Queipo-Ortuño, M. I. (2020). Gut microbiota-mediated inflammation and gut permeability in patients with obesity and colorectal cancer. International Journal of Molecular Sciences, 21(18), 6782. https://doi.org/10.3390/ijms21186782

[28] Scalavino, V., Piccinno, E., Bianco, G., Schena, N., Armentano, R., Giannelli, G., & Serino, G. (2022). The increase of miR-195-5p reduces intestinal permeability in ulcerative colitis, modulating tight junctions' expression. International Journal of Molecular Sciences, 23(10), 5840. https://doi.org/10.3390/ijms23105840

[29] Shi, D., Cui, Y., Liang, H., Wei, Q., Huang, J., & Cao, J. (2026). Gut microbiota-derived tryptophan metabolite indole-3-carboxaldehyde enhances intestinal barrier function via aryl hydrocarbon receptor/AMP-activated protein kinase signaling activation. Animal Bioscience, 39(1), 250225. https://doi.org/10.5713/ab.25.0225

[30] Slifer, Z. M., & Blikslager, A. T. (2020). The integral role of tight junction proteins in the repair of injured intestinal epithelium. International Journal of Molecular Sciences, 21(3), 972. https://doi.org/10.3390/ijms21030972

[31] Wang, K., Wang, H., Lou, W., Ma, L., Li, Y., Zhang, N., Wang, C., Li, F., Awais, M., Cao, S., She, R., Fu, Z. F., & Cui, M. (2018). IP-10 promotes blood–brain barrier damage by inducing tumor necrosis factor alpha production in Japanese encephalitis. Frontiers in Immunology, 9, 1148. https://doi.org/10.3389/fimmu.2018.01148

[32] Wang, X., Zhang, R., Gu, L., Zhang, Y., Zhao, X., Bi, K., & Chen, X. (2015). Cell-based screening identifies the active ingredients from traditional Chinese medicine formula Shixiao San as the inhibitors of atherosclerotic endothelial dysfunction. PLOS ONE, 10(2), e0116601. https://doi.org/10.1371/journal.pone.0116601

[33] Wang, X., Zhao, X., Gu, L., Zhang, Y., Bi, K., & Chen, X. (2014). Discrimination of aqueous and vinegary extracts of Shixiao San using metabolomics coupled with multivariate data analysis and evaluation of anti-hyperlipidemic effect. Asian Journal of Pharmaceutical Sciences, 9(1), 17–26. https://doi.org/10.1016/j.ajps.2014.01.002

[34] Wei, X., Gao, M., Sheng, N., Yao, W., Bao, B., Cheng, F., Cao, Y., Yan, H., Zhang, L., Shan, M., & Chen, P. (2023). Mechanism investigation of Shi-Xiao-San in treating blood stasis syndrome based on network pharmacology, molecular docking and in vitro/vivo pharmacological validation. Journal of Ethnopharmacology, 301, 115746. https://doi.org/10.1016/j.jep.2022.115746

[35] Xiao, Y.-T., Yan, W.-H., Cao, Y., Yan, J.-K., & Cai, W. (2016). Neutralization of IL-6 and TNF-α ameliorates intestinal permeability in DSS-induced colitis. Cytokine, 83, 189–192. https://doi.org/10.1016/j.cyto.2016.04.011

[36] Yue, D., Zheng, Z., Fan, W., Zhu, L., Lin, D., Lu, M., Ji, W., Cao, P., Sun, X., & Hu, C. (2022). Effect of Shixiao San on inflammatory factors and pain in rats with endometriosis. Journal of Ethnopharmacology, 290, 115121. https://doi.org/10.1016/j.jep.2022.115121

[37] Zhang, B., Wei, X., Ding, M., Luo, Z., Tan, X., & Zheng, Z. (2022). Daidzein protects Caco-2 cells against lipopolysaccharide-induced intestinal epithelial barrier injury by suppressing PI3K/AKT and P38 pathways. Molecules, 27(24), 8928. https://doi.org/10.3390/molecules27248928